Semileptonic decay of heavy flavor mesons

Xian-Wei Kang
Beijing Normal University

Based on EPJC2017, EPJC2018, PRD2020, JHEP2021, PRD2022

FB23, Beijing, Sep. 22-27, 2024

- Introduction

- Theoretical tool: quark model with inclusion of relativistic effect

- physical observables

Introduction

- Extraction of CKM matrix element

  compared to pure hadronic decay, clean

  compared to pure leptonic decay, larger Br

  e.g. $B \to e\, \nu_e$ helicity suppression

- Experimental side, huge data sample

  Belle, LHCb, BES, STCF

- Form factor is crucial, related to understanding of QCD

Experimental status

Eur. Phys. J. C 78 (2018) 11, 909

	current	planned
D^+D^-	$(8.296 \pm 0.031 \pm 0.064) \times 10^6$	$\sim 5 \times 10^7$
$D^0\bar{D}^0$	$(10.597 \pm 0.028 \pm 0.087) \times 10^6$	$\sim 6.4 \times 10^7$
$D_s\bar{D}_s$	$\sim 3.3 \times 10^6$	$\sim 2 \times 10^7$

TABLE I. The total numbers of D^+D^-, $D^0\bar{D}^0$, $D_s^+D_s^-$ pairs from BESIII collaboration, where in the data-taking plan the future data samples will be 6 times as large as the current ones. The number of $D\bar{D}$ pair is from Ref. [27].

	Belle	BelleII
$B\bar{B}$	$(7.72 \pm 0.11) \times 10^8$	$\sim 3.9 \times 10^{10}$
$B_s\bar{B}_s$	$(6.53 \pm 0.66) \times 10^6$	$\sim 3.3 \times 10^8$

TABLE II. The total numbers of $B\bar{B}$ and $B_s^+B_s^-$ pairs from Belle collaboration, while BelleII will have the data samples of 50 times as large as Belle by the mid of next decade. The number of $B\bar{B}$ and $B_s\bar{B}_s$ pairs for Belle collaboration are from Refs. [15, 16].

Form factor: general Lorentz structure

$$\mathcal{M}(D_{(s)} \to P(V)\ell\nu_\ell) = \frac{G_F}{\sqrt{2}} V_{cq} H^\mu L_\mu,$$

where $L_\mu = \bar{\nu}_\ell \gamma_\mu (1-\gamma_5)\ell$ and $H^\mu = \langle P(V)|\bar{q}\gamma_\mu(1-\gamma_5)c|D_{(s)}\rangle$.

- For $D_{(s)}$ transitions to pseudoscalar P (π, K, η, η') mesons

$$\langle P(p_P)|\bar{q}\gamma^\mu c|D_{(s)}(p_{D_{(s)}})\rangle = f_+(q^2)\left[p^\mu_{D_{(s)}} + p^\mu_P - \frac{M^2_{D_{(s)}} - M^2_P}{q^2}\, q^\mu\right] + f_0(q^2)\frac{M^2_{D_{(s)}} - M^2_P}{q^2}\, q^\mu,$$

$$\langle P(p_P)|\bar{q}\gamma^\mu\gamma_5 c|D_{(s)}(p_{D_{(s)}})\rangle = 0, \longleftarrow \text{Parity conservation} \qquad (16)$$

- For $D_{(s)}$ transitions to vector V $(\rho, \omega, K^*, \phi)$ mesons

$$\langle V(p_V)|\bar{q}\gamma^\mu c|D_{(s)}(p_{D_{(s)}})\rangle = \frac{2iV(q^2)}{M_{D_{(s)}} + M_V}\epsilon^{\mu\nu\rho\sigma}\epsilon^*_\nu p_{D_{(s)}\rho} p_{V\sigma},$$

$$\begin{aligned}\langle V(p_V)|\bar{q}\gamma^\mu\gamma_5 c|D_{(s)}(p_{D_{(s)}})\rangle &= 2M_V A_0(q^2)\frac{\epsilon^*\cdot q}{q^2}\, q^\mu + (M_{D_{(s)}} + M_V)A_1(q^2)\left(\epsilon^{*\mu} - \frac{\epsilon^*\cdot q}{q^2}\, q^\mu\right) \\ &\quad - A_2(q^2)\frac{\epsilon^*\cdot q}{M_{D_{(s)}} + M_V}\left[p^\mu_{D_{(s)}} + p^\mu_V - \frac{M^2_{D_{(s)}} - M^2_V}{q^2}\, q^\mu\right]. \qquad (17)\end{aligned}$$

- all the dynamic information is contained in the form factor. Calculation of form factor is a central task of theorists.

- No full description in QCD theory: various models, typically a limited range of applicability, *and* *a combination of them give a better picture of underline physics*

1. Heavy meson ChPT, large q^2 region, due to soft pion;

2. QCD light cone sum rule for small q^2 region for B->π;

3. Covariant light-front quark model is often used in the space-like region, and then extrapolate to time-like region.

But there exits models that enable predicting the form factor in the whole kinematic region: **relativistic quark model (RQM) introduced below**.

Relativistic Quark Model (RQM)

Ebet, Faustov, Galkin, e.g., refers to 1705.07741

wave function Ψ_{Λ_Q}, which satisfy the relativistic quasipotential equation of the Schrödinger type [8]

$$\left(\frac{b^2(M)}{2\mu_R} - \frac{\mathbf{p}^2}{2\mu_R}\right)\Psi_{\Lambda_Q}(\mathbf{p}) = \int \frac{d^3q}{(2\pi)^3} V(\mathbf{p},\mathbf{q};M)\Psi_{\Lambda_Q}(\mathbf{q}), \tag{1}$$

where the relativistic reduced mass and and the center-of-mass system relative momentum squared on the mass shell are given by

$$\mu_R = \frac{M^4_{\Lambda_Q} - (m_Q^2 - m_d^2)^2}{4M^3_{\Lambda_Q}},$$

$$b^2(M) = \frac{[M^2_{\Lambda_Q} - (m_Q + m_d)^2][M^2_{\Lambda_Q} - (m_Q - m_d)^2]}{4M^2_{\Lambda_Q}}.$$

1. Based on quasipotential approach, 4 dimension reduced to 3 dimension
2. **Wave function is solvable**, not just assume a Gaussian type function

Relativistic effects: (1) negative-energy part of the propagator

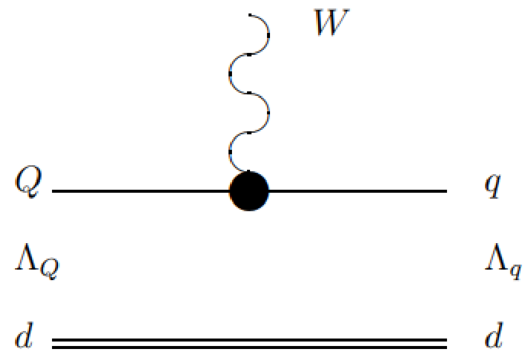

FIG. 1: Lowest order vertex function $\Gamma^{(1)}$ contributing to the current matrix element

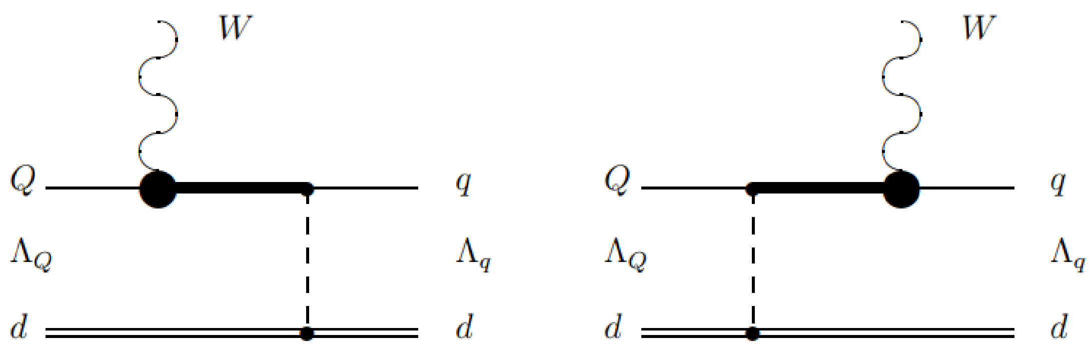

FIG. 2: Vertex function $\Gamma^{(2)}$ taking the quark interaction into account. Dashed lines correspond to the effective potential $\mathcal{V}_{Qd}$ in (3). Bold lines denote the negative-energy part of the quark propagator.

Relativistic effects: (2) wave functions boosted

$$\Psi_{\Lambda\mathbf{P}}(\mathbf{p}) = D_q^{1/2}(R^W_{L_\mathbf{P}})D_d(R^W_{L_\mathbf{P}})\Psi_{\Lambda\mathbf{0}}(\mathbf{p}),$$

where $\Psi_{\Lambda\mathbf{0}}$ is the baryon wave function in the rest frame, R^W is the Wigner rotation, $L_\mathbf{P}$ is the Lorentz boost from the baryon rest frame to a moving one with momentum $\mathbf{P}$, and $D_q^{1/2}(R^W)$ is the rotation matrix of the quark spin [16], while the rotation matrix for the scalar diquark spin $D_d(R^W) = 1$.

Expression for form factor: overlap between initial and final state wave functions

$$\langle\Lambda(P)|J_\mu^W|\Lambda_b(Q)\rangle = \int \frac{d^3p\, d^3q}{(2\pi)^6}\bar{\Psi}_{\Lambda\,\mathbf{P}}(\mathbf{p})\Gamma_\mu(\mathbf{p},\mathbf{q})\Psi_{\Lambda_b\,\mathbf{Q}}(\mathbf{q}),$$

$$\begin{aligned}
f_1^{TV(1)}(q^2) = & -\int \frac{d^3p}{(2\pi)^3}\bar{\Psi}_F\left(\mathbf{p}+\frac{2\epsilon_d}{E_F+M_F}\mathbf{\Delta}\right)\sqrt{\frac{\epsilon_Q(p)+m_Q}{2\epsilon_Q(p)}}\sqrt{\frac{\epsilon_q(p+\Delta)+m_q}{2\epsilon_q(p+\Delta)}}\\
&\times\left\{\frac{\epsilon_d}{E_F+M_F}\left[\frac{M_F}{\epsilon_q(p+\Delta)+m_q}+\frac{M_I}{\epsilon_Q(p)+m_Q}\right.\right.\\
&\left.+\frac{(M_I+M_F)\epsilon_d}{(\epsilon_q(p+\Delta)+m_q)(\epsilon_Q(p)+m_Q)}\frac{E_F-M_F}{E_F+M_F}\right]\\
&+\frac{\mathbf{p\Delta}}{\mathbf{\Delta}^2}\left[\frac{M_F}{\epsilon_q(p+\Delta)+m_q}-\frac{M_I}{\epsilon_Q(p)+m_Q}\right]\\
&\left.-\frac{1}{3}\frac{M_I+M_F}{E_F+M_F}\frac{\mathbf{p}^2}{(\epsilon_q(p+\Delta)+m_q)(\epsilon_Q(p)+m_Q)}\right\}\Psi_I(\mathbf{p});
\end{aligned}$$

$\mathbf{\Delta} = \mathbf{P}-\mathbf{Q};\ \epsilon(p)=\sqrt{m^2+\mathbf{p}^2}$ M_I, M_F mass of initial and final meson

$$|\mathbf{\Delta}| = \sqrt{\frac{(M_I^2+M_F^2-q^2)^2}{4M_I^2}-M_F^2},$$

in the rest frame of mother particle

As it should be, the form factor depends only on q^2

Features of RQM

1. form factor are calculated in the framework of quasipotential approach

2. systematic account of the relativistic effects including transformation of the meson wave function from the rest to the moving frame and contributions of the intermediate negative-energy states.

3**. meson wave functions are taken from previous studies of meson spectroscopy. Parameters have been fixed. Make a prediction for the decay.**

4. **work in the whole range of the transferred momentum q^2**

Semileptonic decays of D and D_s mesons in the relativistic quark model

R. N. Faustov* and V. O. Galkin†
Institute of Cybernetics and Informatics in Education,
FRC CSC RAS, Vavilov Street 40, 119333 Moscow, Russia

Xian-Wei Kang‡
College of Nuclear Science and Technology, Beijing Normal University, Beijing 100875, China

Relativistic description of the semileptonic decays of bottom mesons

R. N. Faustov,[1,*] V. O. Galkin,[1,†] and Xian-Wei Kang[2,3,‡]
[1]*Federal Research Center "Computer Science and Control", Russian Academy of Sciences,*
Vavilov Street 40, 119333 Moscow, Russia
[2]*Key Laboratory of Beam Technology of the Ministry of Education,*
College of Nuclear Science and Technology, Beijing Normal University,
Beijing 100875, China
[3]*Institute of Radiation Technology, Beijing Academy of Science and Technology, Beijing 100875, China*

A full calculation without the heavy quark approximation.

TABLE I: Form factors of the weak D meson transitions.

Decay	Form factor	$F(0)$	$F(q^2_{\max})$	σ_1	σ_2
$D \to K$	f_+	0.716	1.538	0.902	1.07
	f_0	0.716	1.086	0.360	1.657
$D \to K^*$	V	0.927	1.305	0.356	−0.490
	A_0	0.655	1.048	0.432	−0.840
	A_1	0.608	0.660	0.410	0.166
	A_2	0.520	0.623	0.582	−0.917

double-pole form:

$$F(q^2) = \frac{F(0)}{\left(1 - \sigma_1 \frac{q^2}{M^2_{D^*_{(s)}}} + \sigma_2 \frac{q^4}{M^4_{D^*_{(s)}}}\right)},$$

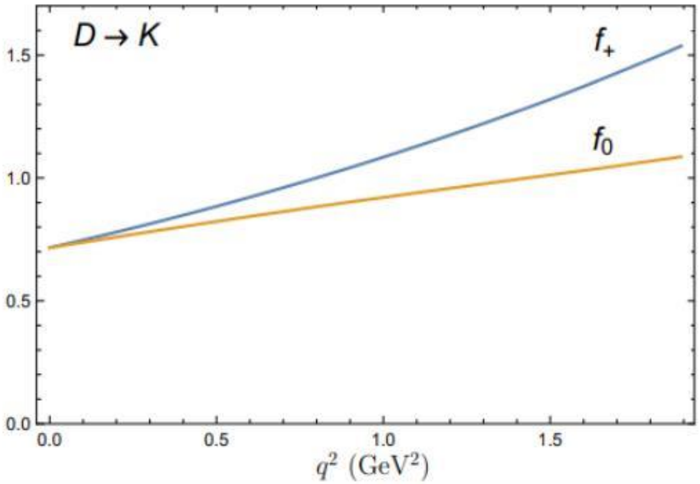

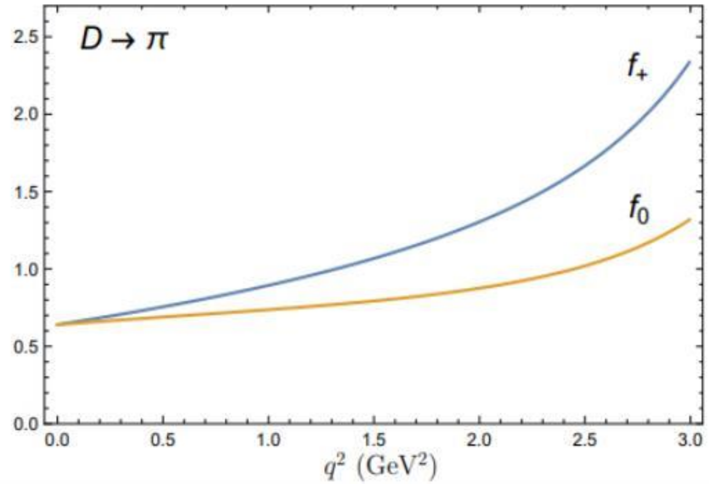

Predictions from covariant light-front quark model.

D->K case not so good, but within 1.5 sigma certainly.

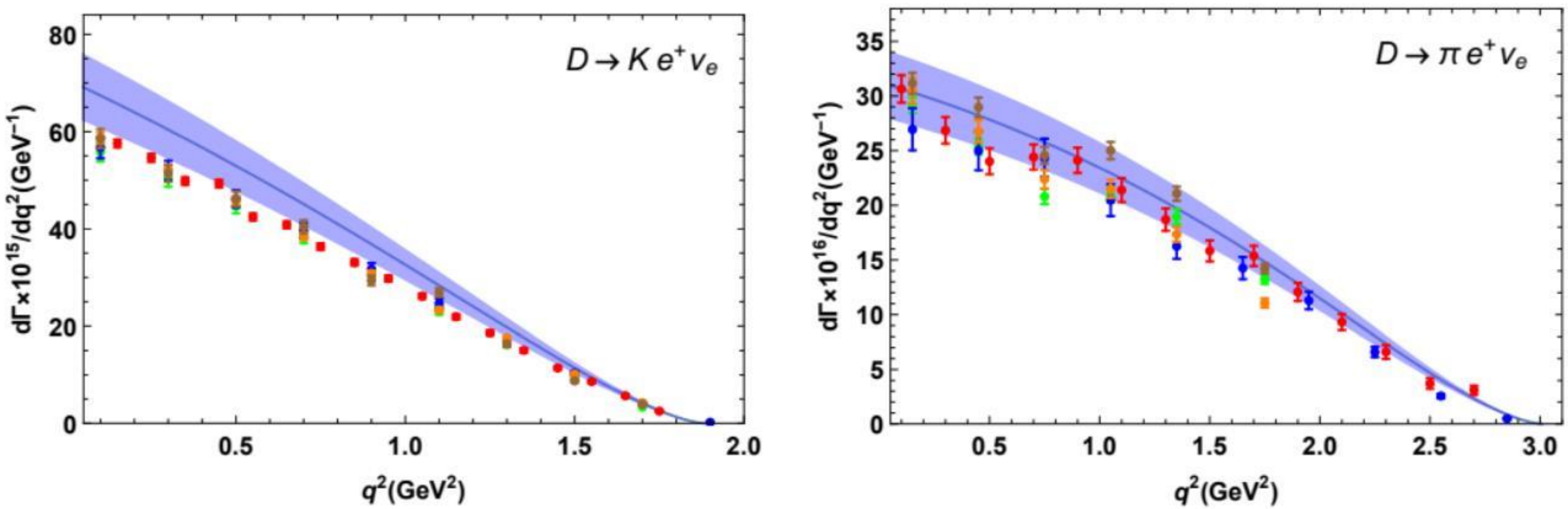

FIG. 4: The differential decay rate for the decays $D \to K e^+ \nu_e$ and $D \to \pi e^+ \nu_e$. The solid line indicates our central values and the band indicates the estimated uncertainty. We have used the experimental data from BES III for neutral D^0 [83] (red dots with error bars) and charged D^+ [50] (green dots with error bars), BaBar [84, 85] (blue dots and error bars) and CLEO [86] for neutral D^0 (orange dots and error bars) and charged D^+ (brown dots with error bars).

Predictions from the relativistic quark model.

All are in agreement nicely.

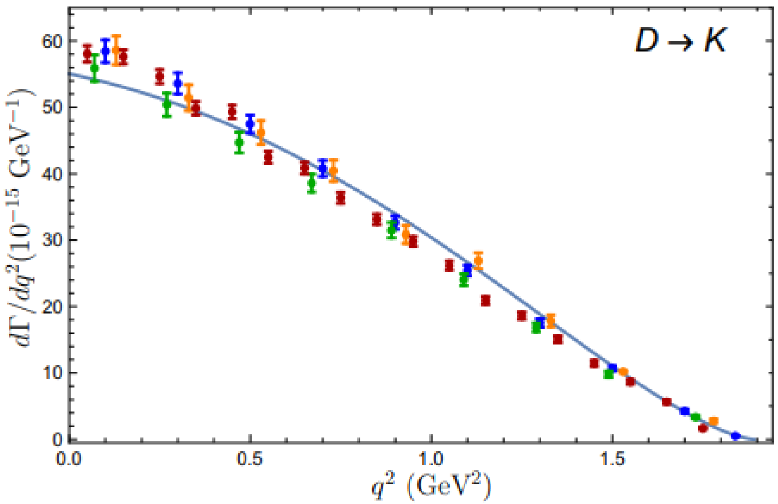

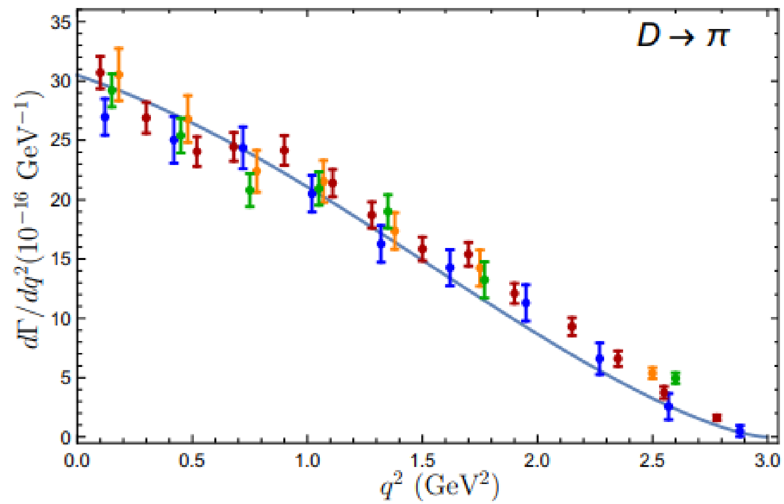

FIG. 4: Comparison of our predictions for the weak $D \to K e \nu_e$ and $D \to \pi e \nu_e$ differential decay rates with experimental data form BaBar [23, 32] (blue dots with error bars), CLEO [33] (orange dots with error bars) and BES III [2, 34] for neutral D^0 (red dots with error bars) and charged D^+ with the account of isospin factor (green dots with error bars) .

Comparison between covariant light-front quark model (CLFQM) and RQM: work in the same way for heavy to heavy transition, but differ for heavy to light transition, which should be due to the different treatment of relativistic effects.

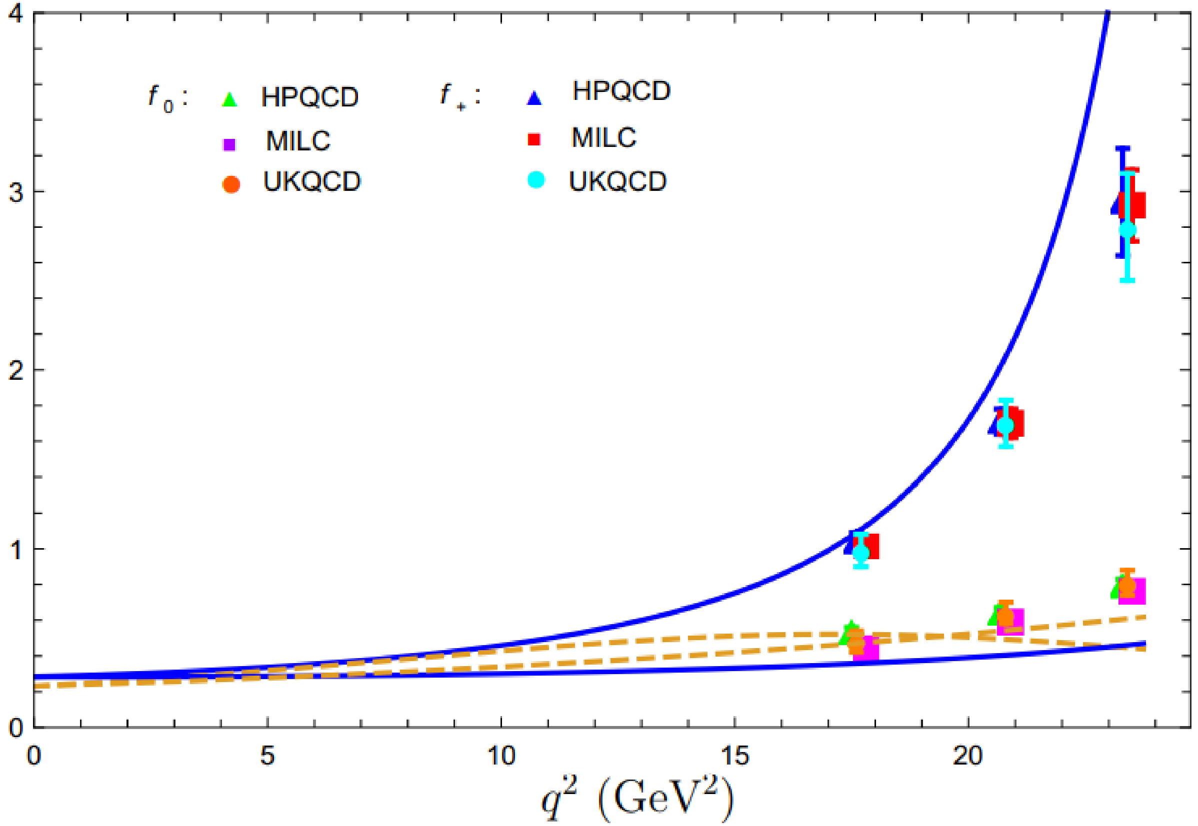

FIG. 2: Same as in Fig. 1, but for the form factors of the weak $B_s \to K$ transitions. For the orange dashed lines, the upper one below $q^2 < 15$ GeV^2 corresponds to $f_+(q^2)$, and the lower one $f_0(q^2)$. HPQCD, MILC and UKQCD data are from Refs. [29], [36] and [32], respectively.

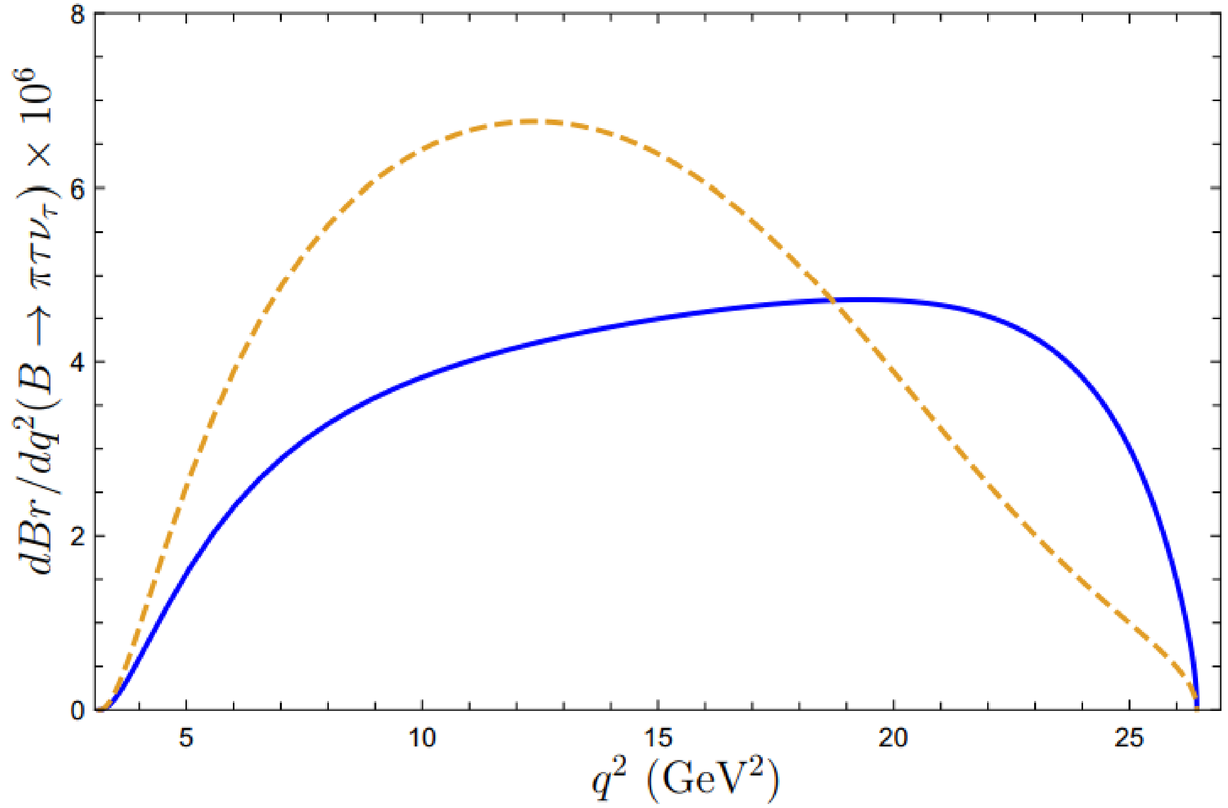

FIG. 4: Differential branching fractions of the semileptonic $B \to \pi\tau\nu_\tau$ decay. Comparison of theoretical predictions (RQM – solid blue lines, CLFQM – orange dashed lines).

To calculate more observables

we exploit the helicity formalism

- conveniently express observables, otherwise may be cumbersome.
- Conveniently work in the partial-wave basis,
often used in the experimental analysis

- The polarization observables are clearly defined.

Virtual W boson has 4 polarization components

orthonormality property

$$\epsilon^{\dagger}_{\mu}(\lambda_W)\epsilon^{\mu}(\lambda'_W) = g_{\lambda_W\lambda'_W}, \quad (\lambda_W, \lambda'_W = t, \pm, 0) \tag{7}$$

and satisfy the completeness relation

$$\epsilon_{\mu}(\lambda_W)\epsilon^{\dagger}_{\nu}(\lambda'_W)g_{\lambda_W\lambda'_W} = g_{\mu\nu}. \tag{8}$$

We can rewrite the contraction of leptonic and hadronic tensors by using the orthonormality and completeness relations as

$$\begin{aligned} L^{\mu\nu}H_{\mu\nu} &= L_{\mu'\nu'}g^{\mu'\mu}g^{\nu'\nu}H_{\mu\nu} \\ &= L_{\mu'\nu'}\epsilon^{\mu'}(\lambda_W)\epsilon^{\dagger\mu}(\lambda''_W)g_{\lambda_W\lambda''_W}\epsilon^{\dagger\nu'}(\lambda'_W)\epsilon^{\nu}(\lambda'''_W)g_{\lambda'_W\lambda'''_W}H_{\mu\nu} \\ &= L\left(\lambda_W, \lambda'_W\right)g_{\lambda_W\lambda''_W}g_{\lambda'_W\lambda'''_W}H\left(\lambda''_W\lambda'''_W\right), \end{aligned} \tag{9}$$

where $L(\lambda_W, \lambda'_W)$ and $H(\lambda_W, \lambda'_W)$ are the leptonic and hadronic tensors in the helicity-component space:

$$L\left(\lambda_W, \lambda'_W\right) = \epsilon^{\mu}(\lambda_W)\epsilon^{\dagger\nu}(\lambda'_W)L_{\mu\nu}, \quad H\left(\lambda_W, \lambda'_W\right) = \epsilon^{\dagger\mu}(\lambda_W)\epsilon^{\nu}(\lambda'_W)H_{\mu\nu}. \tag{10}$$

Calculations of hadronic current and leptonic current are performed in their respective frames!

$D \to P$ transition, we obtain

$$H_t = \frac{1}{\sqrt{q^2}}(m_1^2 - m_2^2)F_0(q^2),$$

$$H_\pm = 0,$$

$$H_0 = \frac{2m_1|\vec{p}_2|}{\sqrt{q^2}}F_1(q^2).$$

the transition $D \to V l^+ \nu_l$:

$$H_t \equiv \epsilon^{\dagger\mu}(t)\epsilon_2^{\dagger\nu}(0)T_{\mu\nu} = -\frac{2m_1|\vec{p}_2|}{\sqrt{q^2}}A_0(q^2),$$

$$H_\pm \equiv \epsilon^{\dagger\mu}(\pm)\epsilon_2^{\dagger\nu}(\pm)T_{\mu\nu} = -(m_1 + m_2)A_1(q^2) \pm \frac{2m_1|\vec{p}_2|}{m_1 + m_2}V(q^2),$$

$$H_0 \equiv \epsilon^{\dagger\mu}(0)\epsilon_2^{\dagger\nu}(0)T_{\mu\nu} = -\frac{m_1 + m_2}{2m_2\sqrt{q^2}}\left(m_1^2 - m_2^2 - q^2\right)A_1(q^2) + \frac{1}{m_1 + m_2}\frac{2m_1^2|\vec{p}_2|^2}{m_2\sqrt{q^2}}A_2(q^2).$$

Branching fraction, as only a number, is not the whole story. Concerning this quantity, all the following model results agree with each other and with experimental numbers.

We need to investigate more observables.

Differential decay rates

Then, we obtain the twofold differential decay distribution on q^2 and $\cos\theta$:

$$\frac{d\Gamma\left(D \to P(V)l^+\nu_l\right)}{dq^2 d\cos\theta} = \frac{G_F^2|V_{cq}|^2|\vec{p}_2|q^2v^2}{32(2\pi)^3m_1^2} \times \left[\left(1+\cos^2\theta\right)\mathcal{H}_U + 2\sin^2\theta\mathcal{H}_L + 2\cos\theta\mathcal{H}_P\right.$$
$$\left.+2\delta_l\left(\sin^2\theta\mathcal{H}_U + 2\cos^2\theta\mathcal{H}_L + 2\mathcal{H}_S - 4\cos\theta\mathcal{H}_{SL}\right)\right].$$

Further integrating over $\cos\theta$, the differential q^2 distribution will be

$$\frac{d\Gamma\left(D \to P(V)l^+\nu_l\right)}{dq^2} = \frac{G_F^2|V_{cq}|^2|\vec{p}_2|q^2v^2}{12(2\pi)^3m_1^2} \times \mathcal{H}_{tot},$$

with $\mathcal{H}_{tot} = \mathcal{H}_U + \mathcal{H}_L + \delta_l\left(\mathcal{H}_U + \mathcal{H}_L + 3\mathcal{H}_S\right)$.

Forward-backward asymmetry

$$\mathcal{A}_{FB}^{l}(q^2) = \frac{\int_0^1 d\cos\theta \frac{d\Gamma}{dq^2 d\cos\theta} - \int_{-1}^{0} d\cos\theta \frac{d\Gamma}{dq^2 d\cos\theta}}{\int_0^1 d\cos\theta \frac{d\Gamma}{dq^2 d\cos\theta} + \int_{-1}^{0} d\cos\theta \frac{d\Gamma}{dq^2 d\cos\theta}} = \frac{3}{4}\frac{H_P - 4\delta_l H_{SL}}{H_{tot}}.$$

The longitudinal polarization of the final charged lepton ℓ is defined as the ratio of the longitudinally polarized decay distribution to the unpolarized decay distribution, Eq . (16) [11, 21]:

$$P_L^\ell(q^2) = \frac{1}{d\Gamma/dq^2}\frac{d\Gamma(s_L)}{dq^2} = \frac{(\mathcal{H}_U + \mathcal{H}_L)\left(1 - \frac{m_\ell^2}{2q^2}\right) - \frac{3m_\ell^2}{2q^2}\mathcal{H}_S}{\mathcal{H}_{\text{total}}}, \tag{21}$$

TABLE XI: Comparison of RQM and CLFQM predictions with lattice data for FB asymmetry and lepton polarization for B decays to light pseudoscalar mesons.

Decay	$\langle A_{FB}\rangle$			$\langle P_L^\ell\rangle$		
	RQM	CLFQM	Lattice [34]	RQM	CLFQM	Lattice [34]
$B \to \pi\mu^+\nu_\mu$	-0.004	-0.005	$-0.0034(31)$	0.99	0.98	0.988(9)
$\bar{B} \to \pi\tau^+\nu_\tau$	-0.22	-0.28	$-0.220(24)$	0.42	0.087	0.301(86)
$\bar{B}_s \to K\mu^+\nu_\mu$	-0.006	-0.007	$-0.0046(28)$	0.98	0.98	0.986(7)
$\bar{B}_s \to K\tau^+\nu_\tau$	-0.24	-0.29	$-0.262(23)$	0.35	-0.10	0.172(91)

There exists only one measurement for the tau longitudinal polarization from Belle. Phys. Rev. Lett. 118 (2017) 211801, with the result of P_L^τ for $\bar{B} \to D^*\tau\upsilon_\tau$ as $-0.38 \pm 0.51^{+0.21}_{-0.10}$.

Polarization observables are very sensitive to different models.
Also used to discriminate the New Physics scenario.

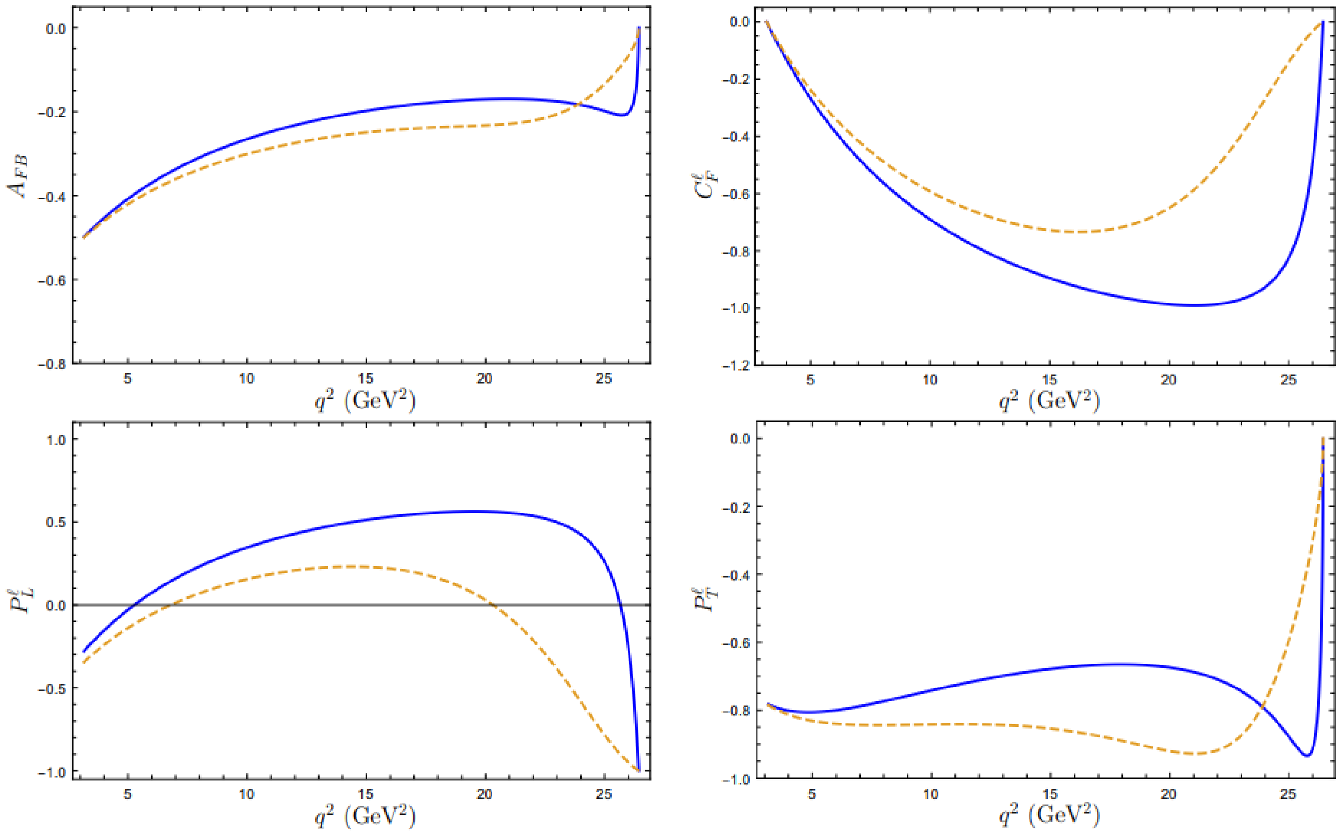

FIG. 5: Comparison of theoretical predictions for the differential FB asymmetry A_{FB} and polarization C_F^ℓ, $P_{L,T}^\ell$ parameters for the semileptonic $B \to \pi\tau^+\nu_\tau$ decay. RQM result are given by blue solid lines and CLFQM results are given by orange dashed lines.

TABLE IX: Ratios of the decay rates with τ and μ leptons $\mathcal{R}(F) = \Gamma(B \to F\tau\nu_\tau)/\Gamma(B \to F\mu\nu_\mu)$ in comparison with available lattice or experimental data, cf. Ref. [3] and references therein.

Transition	Theory			Experiment		
	RQM	CLFQM	Lattice/SM analysis [3]	PDG [1]	HFLAV [40]	[3]
$B \to D$	0.271	0.302	0.298(3)	0.429(82)(52)(B^+)	0.339(26)(14)	0.337(30)
				0.469(84)(53)(B^0)		
$B \to D^*$	0.231	0.246	0.250(3)	0.335(34)(B^+)	0.295(10)(10)	0.298(14)
				0.309(16)(B^0)		
$B \to \pi$	0.631	0.680	0.641(16)			1.05(51)
$B \to \rho$	0.561	0.543	0.535(8)			
$B \to \eta$	0.629	0.611				
$B \to \eta'$	0.544	0.538				
$B \to \omega$	0.566	0.531	0.546(15)			
$B_s \to D_s$	0.287	0.298	0.297(3)			
$B_s \to D_s^*$	0.244	0.248	0.247(8)			
$B_s \to K$	0.588	0.673				
$B_s \to K^*$	0.553	0.520				
$B_c \to \eta_c$	0.373					
$B_c \to J/\psi$	0.284		0.2582(38)	0.71(17)(18)		
$B_c \to D$	0.833					
$B_c \to D^*$	0.656					

Consistency between theories, but may be lower than exp by 1-3 σ

From heavy flavor averaging group. The SM uncertainty is currently subject to debate that HFLAV is following without taking a stance in this.

Experiment	R(D*)	R(D)	Rescaled Correlation (stat/syst/total)
BaBar	0.332 ± 0.024 ± 0.018	0.440 ± 0.058 ± 0.042	-0.45/-0.07/-0.31
BELLE	0.293 ± 0.038 ± 0.015	0.375 ± 0.064 ± 0.026	-0.56/-0.11/-0.50
LHCb	0.336 ± 0.027 ± 0.030	-	-
BELLE	$0.270 \pm 0.035\ ^{+0.028}_{-0.025}$	-	-
LHCb	0.280 ± 0.018 ± 0.029	-	-
BELLE	0.283 ± 0.018 ± 0.014	0.307 ± 0.037 ± 0.016	-0.53/-0.51/-0.51
Average .txt	**0.295 ± 0.011 ± 0.008**	**0.340 ± 0.027 ± 0.013**	**-0.39/-0.34/-0.38**

Thanks for your attention.